Molecular-level carbon traits of fine roots: unveiling adaptation and decomposition under flooded condition

Mengke Wang[1,2,3], Peng Zhang[1,2], Huishan Li[1,2], Guisen Deng[1,2], Deliang Kong[4], Sifang Kong[3], Junjian Wang[1,2]

[1]State Environmental Protection Key Laboratory of Integrated Surface Water-Groundwater Pollution Control, School of Environmental Science and Engineering, Southern University of Science and Technology, Shenzhen 518055, China
[2]Guangdong Provincial Key Laboratory of Soil and Groundwater Pollution Control, School of Environmental Science and Engineering, Southern University of Science and Technology, Shenzhen 518055, China
[3]Department of Transportation and Environment, Shenzhen Institute of Information Technology, Shenzhen 518172, China
[4]College of Forestry, Henan Agricultural University, Zhengzhou 450002, China

Correspondence to: Sifang Kong (mengsiksf@163.com) and Junjian Wang (wangjj@sustech.edu.cn)

Abstract. Fine roots ~~constitute a fundamental source of litter decomposition~~are vital for plant development and ~~humus formation~~carbon biogeochemical cycling in terrestrial ecosystems. ~~However,~~Flooding is known to regulate the physiology and morphology in plant roots; however, its impact on molecular-level characteristics of carbon compounds (carbon traits ~~of carbonaceous organics~~) in fine roots ~~grown in different media, such as soil and water,~~ remain largely unexplored, which limits our understanding of root adaptation and decomposition under changing environments. Here, we used a sequential extraction method, starting from non-polar to polar solvents, to obtain dichloromethane-and-methanol-extractable (F_{DcMe}), base-hydrolyzable (F_{KOHhy}), and CuO-oxidizable (F_{CuOox}) fractions from fine roots of *Dysoxylum binectariferum* naturally grown in soil and water ~~and~~. Subsequently, we characterized them using targeted gas chromatography-mass spectrometry and non-targeted Fourier transform ion cyclotron resonance mass spectrometry. Also, decomposition experiments were conducted on soil- and water-grown roots under aerobic and anoxic conditions. Results showed a consistent increase in unsaturation degree and aromaticity of the analytes from F_{DcMe} to F_{CuOox} fractions. Both analyses were sufficiently sensitive to show that compared to soil-grown roots, the water-grown ones developed more polyphenolics with a high unsaturation degree and aromaticity and had more non-structural compositions. Furthermore, although flooding provided an anoxic condition that slowed down root decomposition, the adaptive strategy of developing more non-structural labile components in water-grown roots accelerated root decomposition, thereby counteracting the effects of anoxia. ~~Our results highlight that the complementary targeted and non-targeted analyses of sequentially extracted fractions can provide the supplementary molecular-level carbon traits of fine roots.~~ It advances our understanding of biogeochemical processes in response to global environmental change.

1 Introduction

Fine roots are an important part of the plant root system owing to their essential functions in resource absorption and transportation (~~Mccormack~~McCormack et al., 2015). Additionally, with the highest productivity and turnover rate among all underground plant organs, fine roots considerably contribute to organic matter formation and stabilization in soils ~~and, thus,~~. Thus, they drive the cycling and distribution of carbon and nutrients in terrestrial ecosystems (Dijkstra et al., 2021). However, the fine-root tissue chemistry is poorly understood (~~Mccormack~~McCormack et al., 2015), significantly hindering our ability to forecast the biogeochemical processes in terrestrial ecosystems accurately.

~~Carbonaceous organic~~Carbon compounds are highly diverse in fine roots. We define fine-root carbon traits as the composition and characteristics of ~~carbonaceous~~carbon compounds in fine roots~~.~~(Freschet et al., 2021a; Freschet et al., 2021b; Wang et al., 2024). The utilization of an extraction method starting from polar to non-polar solvents (Otto and Simpson, 2007) revealed a high level of heterogeneity in ~~carbonaceous~~carbon compounds of fine roots, associated with both root architecture (Wang et al., 2015) and ancestry (Mueller et al., 2012). Additionally, previous studies have elucidated the prominent influence of ~~carbonaceous~~carbon compounds (e.g., terpenes, lignin, and bound phenolics) on root decomposition and, thus, on the terrestrial soil carbon cycling and coevolution between plants and their consumers, microbial symbionts, or humans (Sun et al., 2018; Cornelissen et al., 2023; Augusto and Boca, 2022; Jing et al., 2023). Therefore, identifying the variations in the compositional carbon traits of fine roots is important for predicting the function and fate of fine roots in terrestrial ecosystems.

~~Many pretreatment and extraction methods, such as solvent extraction, base or acid hydrolysis, and alkaline CuO oxidation, have been widely applied in biogeochemistry to infer the source, evolution, and degradation of organic matter (Feng et al., 2008; Wild et al., 2022). Combining these approaches formed sequential extraction methods that selectively break down and extract organic constituents to quantify specific compounds (Otto and Simpson, 2007; Martens, 2002). A small portion of less polar and low molecular weight target compounds, such as dozens of lipids and phenols, can be detected and analyzed using targeted electron ionization gas chromatography mass spectrometry (GC-MS). By comparison, electrospray ionization Fourier transform ion cyclotron resonance mass spectrometry (FT-ICR MS) is a non-targeted technique that has sufficient mass resolving power to separate and accurately assign elemental compositions to individual molecules (He et al., 2022; Qi et al., 2022); it can provide thousands of assigned formulae in sequential chemical extraction from a soil sample (Wang et al., 2022). The application of ultra-high resolution mass accuracy via the FT-ICR MS is expected to advance our understanding of compositional characteristics and the decomposability of fine roots.~~

Global climate change has induced more frequent extreme precipitation and flooding events (Mann et al., 2018), which can cause oxygen deprivation in plants. Roots are directly affected by such events that cause hypoxia and anoxia stress, consequently constraining plant growth and development (Herzog et al., 2016). Fortunately, plants can adapt to hypoxia by changing the morphology and anatomical structure of the root system (Pedersen et al., 2021; Yamauchi et al., 2021), such as

the outgrowth of adventitious roots, the formation of aerenchyma, a higher cortex-to-stele ratio and a lower surface area to volume ratio (Colmer et al., 2019; Yamauchi et al., 2019). The alterations in morphology and anatomy are expected to reflect the inevitable alterations in root tissue chemistry. For example, deoxygenated conditions increase the absolute contents of suberin and lignin in the outer part of the roots in rice (*Oryza sativa* L.) (Kotula et al., 2009). However, unlike the well-documented physiological and morphological plasticity, the molecular-level chemical plasticity in plant roots in flooded environments still lacks a holistic understanding.

The decomposition of plant litter is a fundamental ecosystem process whose rate is known to be regulated by environmental change via reaction kinetics and microbial physiology (Suseela and Tharayil, 2018). Previous studies suggested that flooding causing limitation of oxygen inhibited aerobic respiration of biological communities (Wen et al., 2006) and slowed the rate of litter decomposition (Jessen et al., 2017), resulting in the accumulation of organic carbon and declination of CO_2 flux (Iqbal et al., 2009). In fact, the oxygen requirement of decomposition varies with different chemical compositions in plant litter (Larowe and Van Cappellen, 2011). The labile carbon compounds (profitable energy substances such as carbohydrates, free amino acids, and proteins) are preferably decomposed compared with recalcitrant carbon compounds (complex aromatic bio-polymers such as lignin and suberin) whose decomposition depends strongly on oxygen (Agethen and Knorr, 2018; Kirschbaum et al., 2021). As mentioned above, the flooded environments are expected to alter the chemical composition of root litter and thus indirectly impact decomposition. However, whether this indirect effect strengthens or counteracts the direct effect of anoxia on litter decomposition rate is poorly understood.

Numerous plants naturally thrive at the waterline within tropical forests, offering an exceptional opportunity to examine and verify the responsiveness of plant fine roots to environmental fluctuations. Here, soil-grown (SGR) and water-grown fine roots (WGR) of *Dysoxylum binectariferum* Hook. f., an evergreen plant with medicinal value that is common in China, India, and other parts of Asia (Coffin and Ready, 2019; Bharate et al., 2018), were subjected to a series of extraction and chemical degradation steps and then analyzed using targeted (electron ionization gas chromatography-mass spectrometry, GC-MS) and non-targeted (Fourier transform ion cyclotron resonance mass spectrometry, FT-ICR MS) techniques to determine their molecular signatures. In addition, the residues after each degradation step were analyzed using elemental analysis and solid-state ^{13}C cross-polarization magic angle spinning nuclear magnetic resonance (NMR) to determine the changes in carbon content and bulk molecular composition during the extraction procedures, respectively. ~~We tested three main hypotheses: 1) compared to the targeted analysis, sequential chemical depolymerization combined with FT-ICR MS analysis of the biopolymer-derived organic matter could provide complementary molecular information on root tissue chemistry; 2~~We tested two main hypotheses: 1) compared to SGR, WGR should contain more aromatics, especially in bound-compounds to cope with flooding stress; and ~~3~~2) the WGR would have lower decomposition rate than the SGR in both aerobic and anoxic conditions. This study establishes a comprehensive tool resolving the molecular-level carbon traits of fine roots that will extend knowledge of the possible mechanism underlying the response of the belowground carbon cycling to global environmental change.

2 Materials and methods

2.1 Study site and sample collection

The study site was in a tropical seasonal rain forest in Xishuangbanna (101°25 'E, 21°41' N), southwestern China. The forest receives an average annual precipitation of 1539 mm and has an average annual temperature of 21.5°C. The soils are classified as Oxisols in the soil taxonomy. We collected root samples from three mature trees of *Dysoxylum binectariferum* Hook. f growing by a slow flowing stream, with both roots growing in soil and growing in water (Fig. S1, see Text S1 in the Supplement for more details). At the same time, the soil and sediment near the roots were also collected. All fine roots, soils, and sediments were immediately collected in plastic bags, transported in a cooler to the laboratory, and frozen at –20 °C. Root morphology parameters were acquired by root image analysis using Winrhizo software (2007 Pro version; Regent Instruments, Quebec, QC, Canada). Before chemical analyses, the fine roots were gently cleaned in cool water, freeze-dried, and ground into fine powder.

2.2 Isolation and ~~target~~targeted analysis by GC-MS of individual compounds

The compounds in fine roots were separated into three fractions via sequential extraction (Fig. 1) based on the methods of Otto and Simpson (2007) and Wang et al. (2015), with modifications. Triplicate extractions of each root sample were conducted. Extraction of the roots with organic solvents followed by alkaline hydrolysis can obtain the free compositions (such as free lipids, steroids, and carbohydrates) and ester-bound compositions (cutin and suberin monomers), respectively. The CuO oxidation yields ether-bonded compositions (preferentially lignin phenols). Briefly, solvent extraction by dichloromethane (DCM), methanol (MeOH): DCM (1:1, v/v), and MeOH consecutively for the dichloromethane and methanol extractable fraction (F_{DcMe}) was performed with homogenized root samples (R1). The root residues (R2) after solvent extraction were hydrolysed with 1 mol·L^{-1} methanolic KOH (100°C, 3 h) for the base-hydrolyzable fraction (F_{KOHhy}). Dried root residues (R3) were further subjected to alkaline cupric oxide (CuO) oxidation with CuO, $Fe(NH_4)_2(SO_4)_2 \cdot 6H_2O$, and 1 mol·L^{-1} NaOH for the CuO-oxidizable fraction (F_{CuOox}). The isolated individual compounds were ~~derivatization~~derivatized before GC-MS analysis using an Agilent 7890B gas chromatograph equipped with a 5977B mass spectrometer. Further details are given as Text S2 in the Supplement.
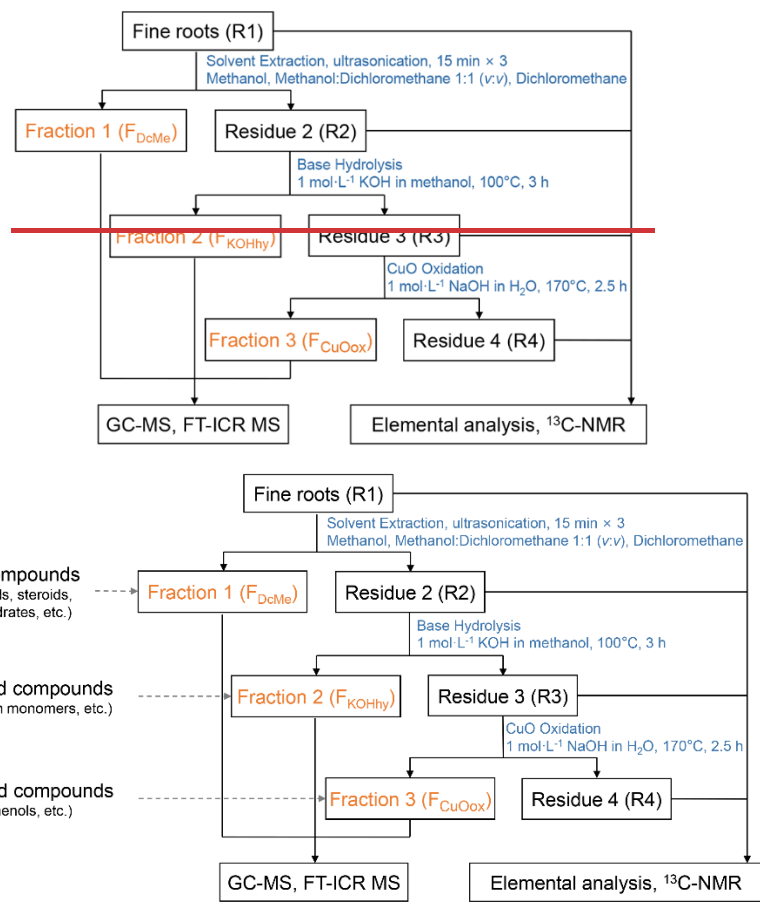
Figure 1 Schematic chart of the sequential extraction of organic compounds from fine roots to obtain different operational fractions and residues. GC-MS: gas chromatography-mass spectrometry; FT-ICR MS: Fourier transform ion cyclotron resonance mass spectrometry; ^{13}C-NMR: ramp solid-state ^{13}C cross-polarization magic angle spinning nuclear magnetic resonance. F_{DcMe}: dichloromethane and methanol extractable fraction; F_{KOHhy}: base-hydrolyzable fraction; and F_{CuOox}: CuO-oxidizable fraction.

2.3 FT-ICR MS analysis and molecular formula assignment

Aliquots of the extracts (F_{DcMe}, F_{KOHhy}, and F_{CuOox}) were dissolved in MeOH at a target carbon concentration of approximately 50 µg·mL^{-1}. The solution was infused into a 9.4 Tesla Bruker Apex-Ultra FT-ICR MS (Bruker, Germany) using the ESI mode for ionization. Signals were accumulated with 128 scans, a 2 M word size, and a mass range of m/z 200–800.

Mass peaks were internally calibrated with a target mass measurement accuracy of < 1.0 ppm. The thresholds of signal-to-noise and absolute intensity for peak selection were set as 7 and 100, respectively. Following the compound identification algorithm (Kujawinski and Behn, 2006), elemental formulae were assigned using the Formularity software (Tolić et al., 2017), with the additional requirements of $^{12}C_{1-60}$, $^{1}H_{1-120}$, $^{14}N_{0-3}$, $^{16}O_{0-30}$, and $^{32}S_{0-1}$. The double-bond equivalent (DBE),

modified aromaticity index (AI_{mod}), and nominal oxidation state of carbon (NOSC) were calculated to reveal the degrees of unsaturated states (Koch and Dittmar, 2006, 2016), aromaticity (Koch and Dittmar, 2006, 2016), and relative nominal oxidation state of organic matter (Kellerman et al., 2015), respectively. Furthermore, the unique formulae in SGR and WGR were identified and analyzed based on Kendrick mass defect (KMD) plots to display the reaction trends of (1) hydrogenation/dehydrogenation (H_2 series), (2) methylation/demethylation (CH_2 series), (3) ring-opening reactions (O_2 series), and (4) carboxylation/decarboxylation (COO series) (Waggoner and Hatcher, 2017; Khatami et al., 2019).

2.4 Solid-state ^{13}C-NMR analysis

Approximately 100 mg of root sample (R1) or residue after each extraction step (R2, R3, and R4) was packed into a 4 mm zirconium rotor with a Kel-F cap. The solid-state ^{13}C NMR spectra were acquired using a Bruker AVANCE III 600 spectrometer at a resonance frequency of 150.9 MHz, with a 4 mm magic angle spinning probe and spun at 12 kHz. A contact time of 4 ms and a recycle delay of 2 s were used for ramp cross-polarization magic angle spinning NMR measurement. The spectra were divided into seven central resonance regions according to the chemical shift as follows (Nelson and Baldock, 2005): 0–45 ppm for alkyl carbon; 45–60 ppm for *N*-alkyl/methoxy carbon; 60–95 ppm for *O*-alkyl carbon; 95–110 ppm for di-*O*-alkyl carbon; 110–145 ppm for aromatic carbon; 145–165 ppm for *O*-aromatic carbon; and 165–210 ppm for carbonyl and carboxyl carbon. The relative abundance of these seven carbon regions was then calculated.

2.5 Fine root decomposition

Both SGR and WGR were incubated in a mixed matrix of A horizon soil near SGR and surface sediment near WGR under anoxic or aerobic conditions. Before incubation, any visible plant residues and stones with a diameter of > 2 mm were removed from the soil and sediment. Then the soil and sediment were homogenized based on a 1:1 fresh mass ratio. For anoxic conditions, a glass tube (4.5 cm diameter × 10 cm depth) was filled with 100 g of the freshly mixed matrix (65 g in dry weight) and 80 mL of deionized water (5 cm of overlying water). For aerobic conditions, the fresh mixture matrix was air dried to 60% water holding capacity (WHC) and then filled into another glass tube (65 g in dry weight). Anoxic and aerobic incubation experiments of the SGR and WGR were set up with three replicates, which resulted in 12 microcosms in total. Then, 1 g of freeze-dried root sample was sealed in a clean polyamide litterbag (3.5 × 7 cm, 40 μm mesh). All litterbags were completely buried in microcosms and closely contacted with the mixed soil and sediment matrixes. The experimental microcosms were kept in a dark incubator at 25 °C. The mixed matrixes in aerobic condition were held at 60% WHC, and those in anoxic condition were held with 5 cm of overlying water via weekly additions of deionized water. All microcosms were harvested after 180 days. After that, decomposed fine roots were collected, cleaned, and freeze-dried, after which they were weighed and ground for carbon content analysis.

2.6 Statistical analysis

The results of targeted analyses were statistically evaluated by analysis of variance (ANOVA) to reveal differences in one or
more discrete variables (IBM SPSS Statistics 23). Statistical difference was considered when $P < 0.05$.

Significant differences in the chemical characteristics between SGR and WGR were assessed using a two-way independent-samples t-test. Furthermore, significant differences among the three fractions were analysed using a two-way analysis of variance (ANOVA) followed by Tukey's post hoc test for pairwise comparisons. All statistical analyses were conducted using IBM SPSS Statistics 23. Statistical difference was considered when $P < 0.05$.

3 Results

3.1 Biomass and carbon fractions in sequential extraction steps

Each sequential extraction step could extract considerable proportions of biomass and carbon for all root samples. F_{KOHhy}
after base hydrolysisand F_{CuOox} had the similar ($P > 0.05$) and highest biomass fractionfractions, accounting for over one-third34% and 32% of the total biomass, respectively, while F_{DcMe} had the lowest biomass fraction with approximately 10%
of the total biomass (Fig. 2a; Table S1). There was approximately one quarter24% of biomass residue after the three-step extraction. Regarding the chemical element composition, nearly 90% of carbon was extracted via the three-step chemical extraction, and more than 70% of carbon was evenly distributed in F_{KOHhy} and F_{CuOox} (Fig. 2b). Compared with SGR,; Table S1). Although WGR had 74% morenear twice biomass and a 96% higher carbon fractionfractions in F_{DcMe} of SGR ($P < 0.05$), the two classes of roots were similar on both biomass and carbon content in the other three fractions ($P > 0.05$; Table S1). The proportion of ash content in SGR was approximately twice that in WGR ($P < 0.05$; Fig. 2c; Table S1).

(a) Biomass fractionation

dichloromethane and methanol extractable fractions (F_{DcMe})

base-hydrolyzable fractions (F_{KOHhy})

CuO-oxidizable fractions (F_{CuOox})

Residue after CuO oxidation

(b) Fractional carbon contents
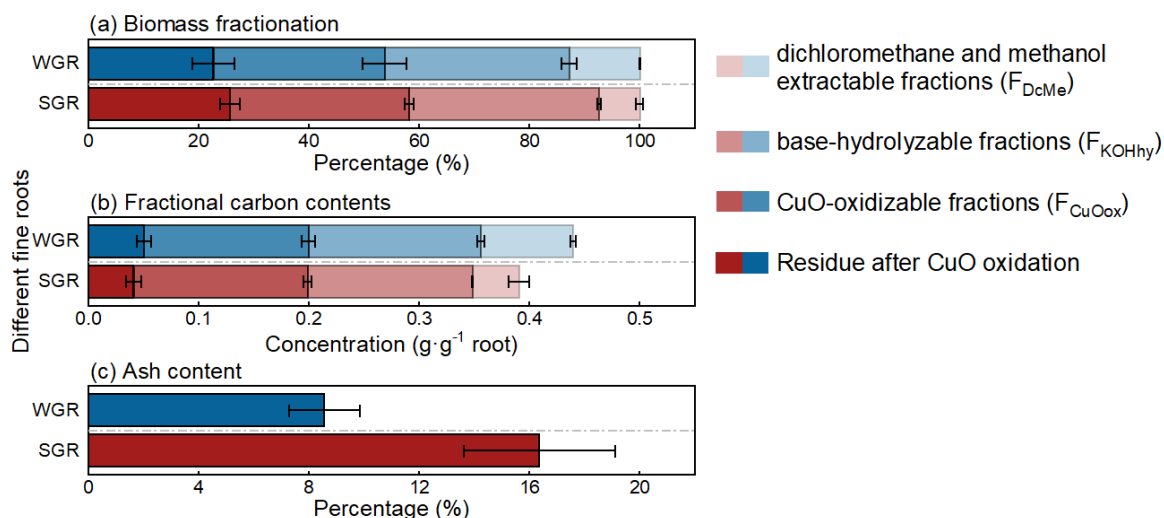
(c) Ash content

Figure 2 Average biomass fractionation (**a**) and fractional carbon contents (**b**) based on sequential extraction and ash content (**c**) of water-grown (*WGR*, blue bar) or soil-grown roots (*SGR*, red bar). Four colors, from light to dark, indicate the dichloromethane and methanol extractable fraction (F_{DcMe}), base-hydrolyzable fraction (F_{KOHhy}), CuO oxidizable fraction (F_{CuOox}), and residue after CuO oxidation. Bars represent means ± standard errors (n = 3).

Solid-state ^{13}C NMR spectroscopy showed the variations in carbon structure in different extracted fine root residues (Fig. 3, Fig. S2). After solvent extraction, the intensity of the alkyl carbon region significantly decreased ($P < 0.05$) in all fine-root samples. Base hydrolysis significantly reduced the signal intensity in the carbonyl and carboxyl carbon region in SGR and the *O*-aromatic carbon region in WGR ($P < 0.05$), which indicated that these structures were extracted by base hydrolysis. The carbonyl and carboxyl, and aromatic carbon regions in SGR decreased after CuO oxidation, as did the carbonyl and carboxyl, and *N*-alkyl/methoxy C regions in WGR ($P < 0.05$).
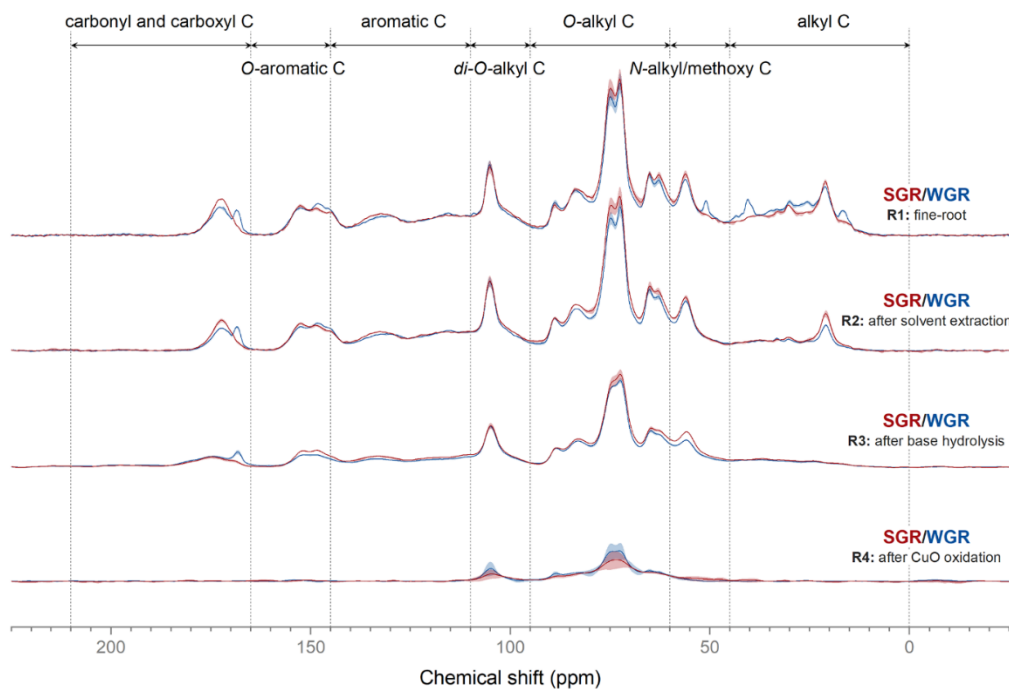
Figure 3 Solid-state ^{13}C cross-polarization magic angle spinning nuclear magnetic resonance spectra of fine-root samples (R1) and the residues after dichloromethane and methanol extraction (R2), base hydrolysis (R3), and CuO oxidation (R4). The shadow areas represent the range of means ± standard errors (n = 3).

3.2 Composition based on GC-MS analyses

The dichloromethane and methanol extractable fractions (F_{DcMe}) contained more than 70 compounds detected by GC-MS and identified by comparing mass spectra with the NIST library (Table ~~S1~~S2). Based on their functions, chemical characteristics, and specificities, according to Macabuhay et al. (2022), these compounds in F_{DcMe} were subdivided into six principal categories—phenolics, glycerolics, prenolics, carbohydrates, fatty acyls, and steroids (Fig. 4a). The total concentration of

these compounds in F_{DcMe} reached approximately 100 mg g ~~C~~OC^{-1} in all fine roots. Compared with SGR, WGR had significantly more phenolics ($P = 0.007$), prenolics ($P < 0.001$), steroids ($P < 0.001$), and total lipids ($P = 0.001$) but less glycerolics ($P = 0.001$), carbohydrates ($P = 0.056$), and fatty acyls ($P = 0.028$).

The base-hydrolyzable fractions (F_{KOHhy}) yielded 23 aliphatic and 15 phenolic compounds (Table ~~S1~~S2), with a total concentration of 20–30 mg g ~~C~~OC^{-1} in all fine roots (Fig. 4b). The aliphatic compounds predominantly comprised even-numbered, mid- to long-chain homologs (C_{10}–C_{26}) of x- and ω-hydroxyalkanoic acids (x-/ω-OH acids), n-alkanols, saturated normal fatty acids (FAs), saturated normal fatty diacids (DAs), and unsaturated normal fatty acids (UAs). Compared with SGR, WGR was significantly enriched in more phenolics ($P < 0.001$) but in fewer aliphatics ($P = 0.022$).

Ten phenols (total concentration of 27 ± 5 mg g ~~C~~OC^{-1}) were the predominant products in F_{CuOox} after CuO oxidation, with *CAD* not detected (Fig. 4c; Table ~~S2~~S3). The eight lignin phenols (except *PAL*, *PON*, and *PAD*) amounted to 24 ± 5 mg g ~~C~~OC^{-1} of the root samples. Of these phenols, vanillyl phenols (*VAL*, *VON*, and *VAD*) were the main components accounting for more than 60% of all phenols, followed by syringyl phenols (*SAL*, *SON*, and *SAD*) that accounted for over 20% of the total concentration. The roots from different growing media differed in the composition of monomeric phenols. Compared with SGR, WGR had more p-hydroxyl phenols ($P = 0.047$) and vanillyl phenols ($P = 0.072$) and exhibited higher values of acid-to-aldehyde ratios of vanillyl and syringyl phenols (i.e., $(Ad:Al)_V$ and $(Ad:Al)_S$; $P = 0.056$ and $P = 0.020$, respectively) but lower syringyl-to-vanillyl ratio ($S:V$) values ($P = 0.002$) (Table ~~S2~~S3).
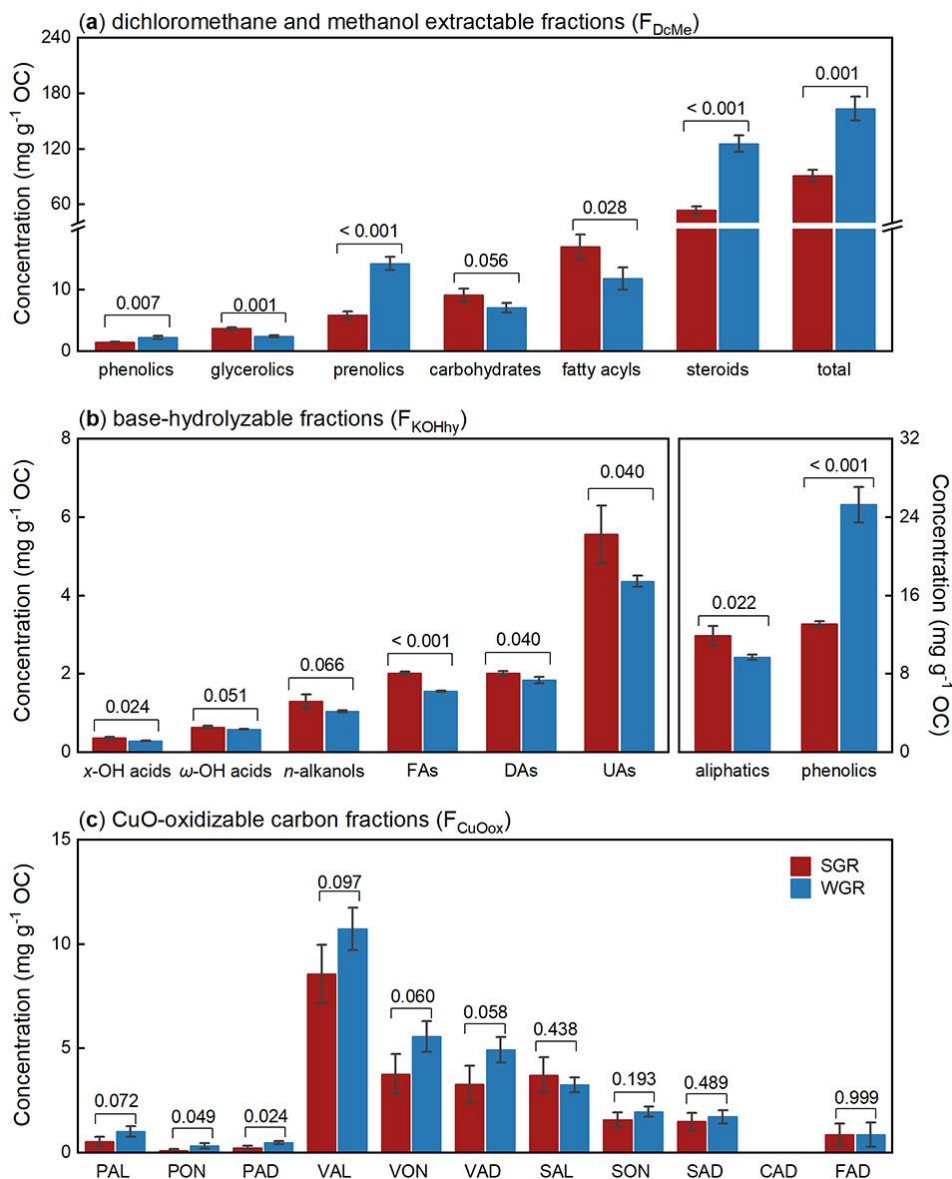
Figure 4 Molecular-level compositions of dichloromethane and methanol extractable fractions (F_{DcMe}) (**a**), base-hydrolyzable fractions (F_{KOHhy}) (**b**), and CuO-oxidizable fractions (F_{CuOox}) (**c**) of soil-grown roots (SGR, in red) and water-grown roots (WGR, in blue). The Y axes represent organic carbon (OC)-normalized concentrations. Bars represent mean ± standard error (n = 3). The coefficient above each pair of bars is the *P*-value of two-~~tailed~~way *t*-test analyses of the significant differences between SGR and WGR. *x*-/*ω*-OH acids: *x*- or *ω*-hydroxyalkanoic acids; FAs: saturated normal fatty acids; DAs: saturated normal fatty diacids; UAs: unsaturated normal fatty acid; PAL: *p*-hydroxybenzaldehyde; PON: *p*-hydroxyacetophenone; PAD: *p*-hydroxybenzoic acid; VAL: vanillin; VON: acetovanillone; VAD: vanillic acid; SAL: syringaldehyde; SON: acetosyringone; SAD: syringic acid; CAD: *p*-coumaric acid; and FAD: ferulic acid. Detailed concentration data of individual compounds are shown in Table ~~S1~~S2.

3.3 Molecular composition based on FT-ICR MS analyses

The FT-ICR MS spectra of all samples provided 8631 assigned formulae (Fig. S3; Table ~~S3~~S4). From F_{DcMe} to F_{CuOox}, the average H/C ratio (weighed by peak intensity) continuously decreased, and the average O/C ratio, DBE, AI_{mod}, and NOSC continuously increased ($P < 0.05$) (Table ~~S4~~S5), demonstrating the increasing unsaturation degree and aromaticity. In the three fractions, the formulae containing only carbon, hydrogen, and oxygen (CHO) accounted for more than half of the total number and nearly 90% of the total abundance of all assigned formulae (Table ~~S4~~S5). In addition, there was a considerable quantity of nitrogen- or/and sulfur-containing compounds (CHON, CHOS, and CHONS), but these only accounted for approximately one-tenth of the total formulae abundance. Compared with SGR, WGR had a higher average O/C ratio, DBE, AI_{mod}, and NOSC and a lower average H/C ratio ($P < 0.05$) (Table ~~S4~~S5), which represented higher unsaturation degree and aromaticity in WGR. However, there were lower proportions of sulfur-containing compounds (CHOS and CHONS) in WGR than in SGR.

The common formulae in all three replicates covered an average of 76% and 90% of the total number and signals in a replicate, respectively (Fig. S3; Table ~~S3~~S4), and thus had strong molecular characteristic representativeness. A total of 4368 common formulae (2500 in F_{DcMe}, 2070 in F_{KOHhy}, and 4214 in F_{CuOox}) in the three SGR replicates and 3461 (2594 in F_{DcMe}, 1962 in F_{KOHhy}, and 1746 in F_{CuOox}) in the three WGR replicates were identified (Fig. S4). The number of co-existing formulae in the three fractions (F_{DcMe}, F_{KOHhy}, and F_{CuOox}) accounted for approximately 30% of the total formulae in both SGR and WGR. More aromatic formulae with low average H/C ratios and high average O/C ratios were present in the F_{CuOox} of SGR and F_{KOHhy} and F_{CuOox} of WGR than that in the F_{DcMe} (Fig. 5; Fig. S4). Compared with SGR, WGR had more formulae with high O/C ratios and low H/C ratios in specific and common formulae in the three fractions (Fig. 5).

245
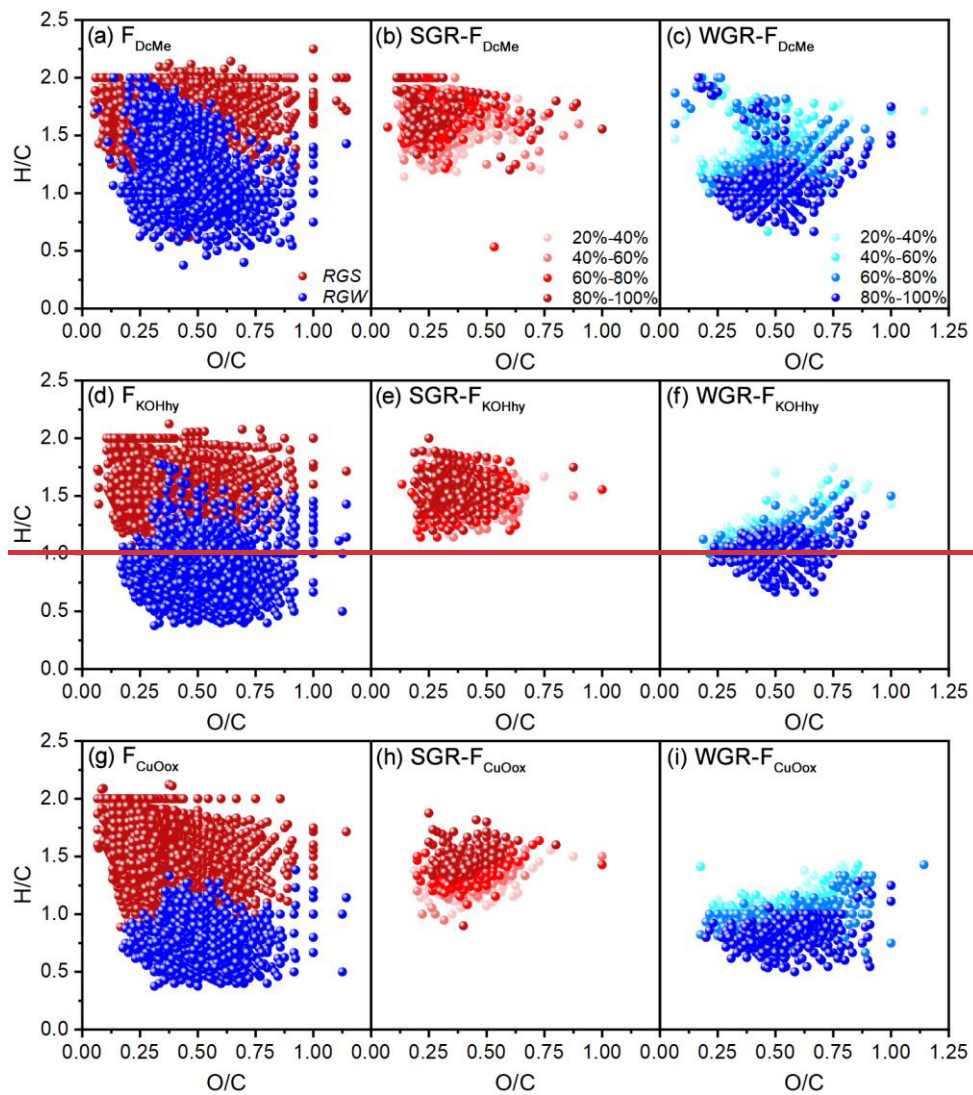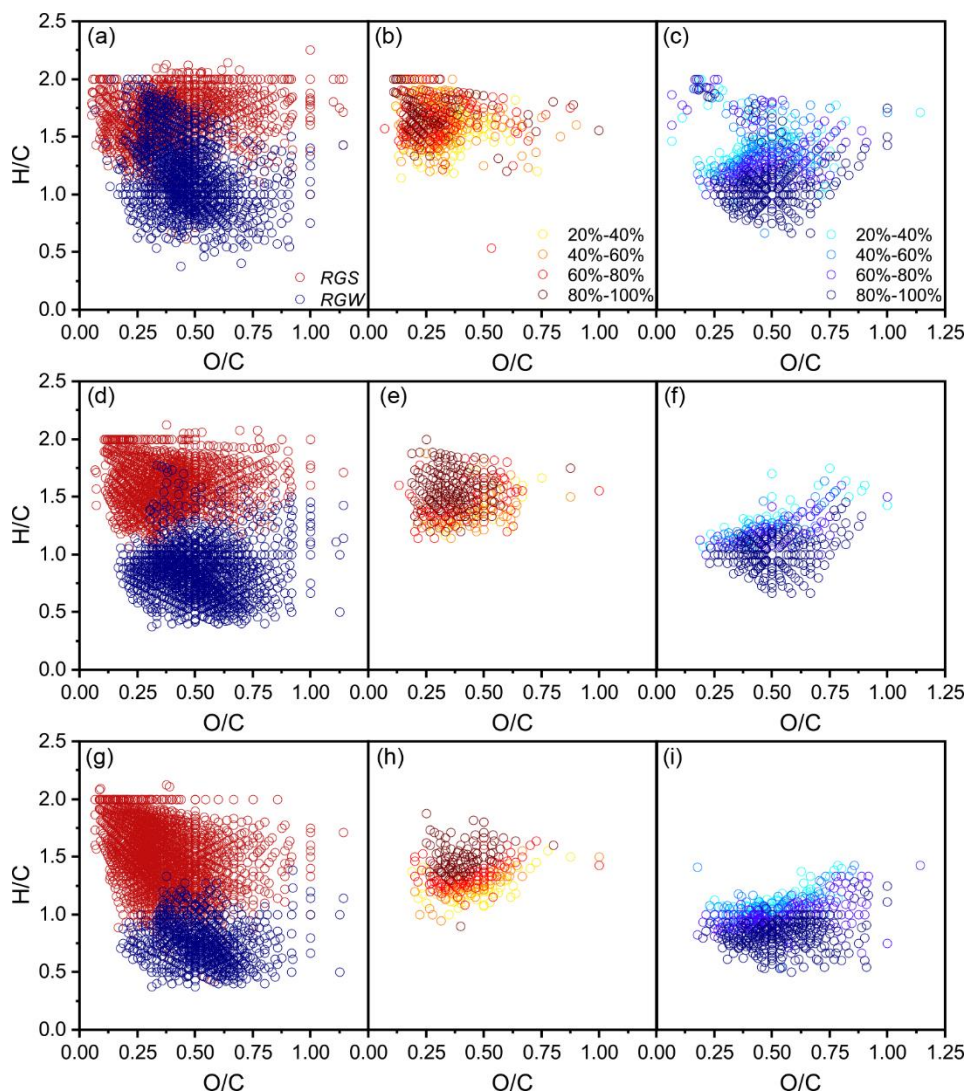
Figure 5 Comparison of van Krevelen diagrams for Fourier transform ion cyclotron resonance mass spectrometry (FT-ICR MS)-detected specific formulae of soil-grown roots (SGR, in red) and water-grown roots (WGR, in blue) from (**a**) dichloromethane and methanol extractable fractions (F_{DcMe}), (**d**) base-hydrolyzable fractions (F_{KOHhy}), and (**g**) CuO-oxidizable fractions (F_{CuOox}). van Krevelen diagrams of formulae that are common but have higher relative abundance in SGR ~~(b, e, h)~~ than in WGR (b, e, h) or higher relative abundance in WGR than in SGR (**c, f, i**).

Kendrick mass defect (KMD) plots showed a unimodal clustering of KMD plotted against *m/z* stretching from the molecular formulas with high KMD for aliphatics to those with low KMD for aromatics (Fig. 6). A considerable number of new molecules existed in WGR compared with SGR, which exhibited a definite shift towards lower *m/z* values for the KMD CH_2 and KMD H_2 series (Fig. 6a-f) and higher *m/z* values for the KMD O_2 and KMD COO series (Fig. 6g-l). The results

suggested the oxidation of aliphatic chains and aromatic rings, as well as the ring opening of aromatic rings and carboxylation of new molecules in WGR.
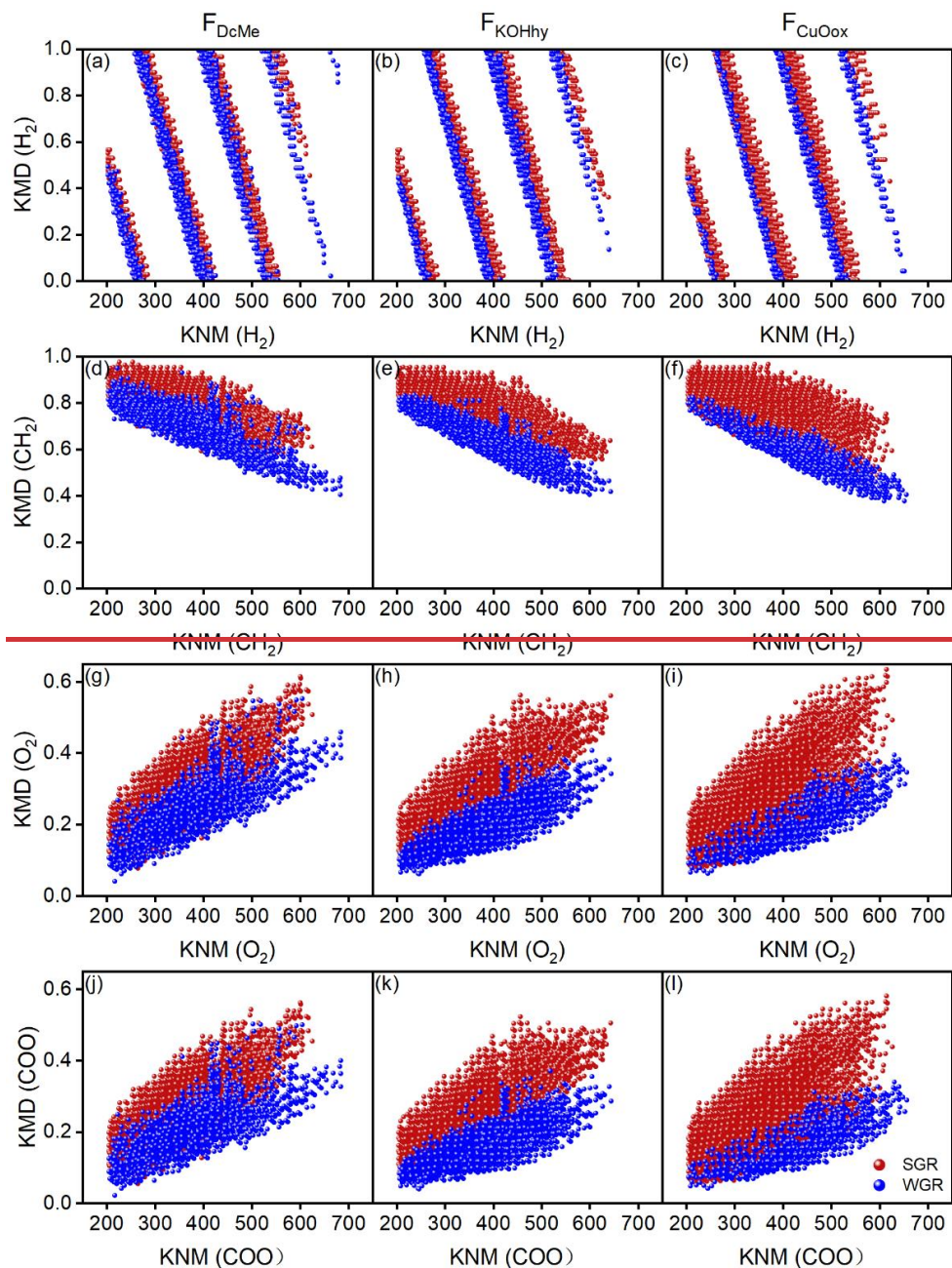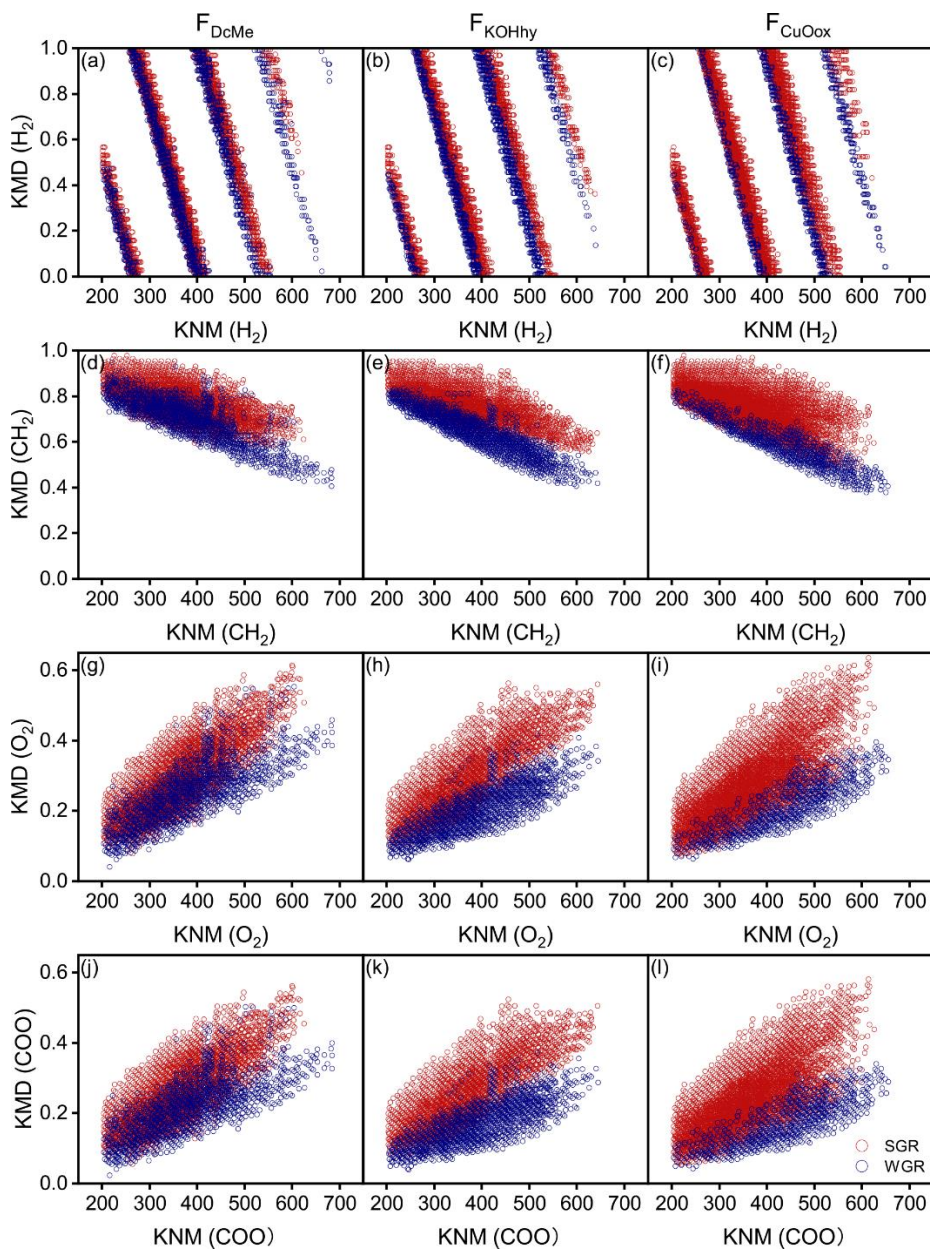
Figure 6 Kendrick mass defect (KMD) plots for Fourier transform ion cyclotron resonance mass spectrometry (FT-ICR MS)-detected specific formulae of soil-grown roots (SGR, in red) and water-grown roots (WGR, in blue) from (**a**, **d**, **g**, **j**) dichloromethane and methanol extractable fractions (F$_{DcMe}$), (**b**, **e**, **h**, **k**) base-hydrolyzable fractions (F$_{KOHhy}$), and (**c**, **f**, **i**, **l**) CuO-oxidizable fractions (F$_{CuOox}$). The four rows display KMD for H$_2$, CH$_2$, O$_2$, and COO series.

3.4 Decomposability of fine roots

265 ~~The two way ANOVA~~To investigate the influencing factors regulating fine-root decomposition, we detected the morphological traits and nitrogen content in origin roots. The results showed that SGR has a higher specific root length and nitrogen content, with a lower average diameter and carbon nitrogen ratio than WGR ($P < 0.05$; Table S6). After 180 days of decomposition, the two-way t-test analyses revealed that redox condition and root source significantly affected the percentage of root carbon remaining ~~after 180 days of decomposition~~ (Table ~~S5~~S7). Both kinds of fine roots had more

270 proportion of carbon remaining in anoxic condition than in aerobic condition (Fig. 7). WGR had 14% and 13% less carbon remaining in aerobic condition ($P = 0.003$) and anoxic condition ($P < 0.001$) than SGR, respectively. Therefore, organic carbon decomposability was consistently higher in WGR than in SGR.
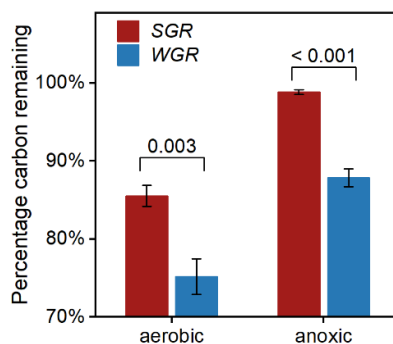
Figure 7 Percentage of carbon remaining of fine roots collected from soil (in red) and water (in blue) after 180 days of decomposition in
275 aerobic and anoxic conditions. Bars represent mean ± standard error (n = 3). The coefficient above each pair of bars is the P-value of two-~~tailed~~way t-test analyses of the significant differences between root sources.

4 Discussion

4.1 Extended information captured by non-targeted analyses of root fractions

Fine roots contain abundant ~~carbonaceous~~carbon compounds with heterogeneous and macromolecular structures. In this
280 study, the biomass and carbon directly extracted using organic solvents only accounted for 11% and 16% of the total biomass and total carbon in roots, respectively (Fig. 2). This indicated that most biomass and carbon were distributed in the non-free biopolymers of roots. Thus, the ~~carbonaceous~~carbon compounds obtained via simple solvent extraction could hardly represent the full characteristics of fine roots. Alkaline hydrolysis is an established method to obtain many ester-bound compounds from organic heteropolymers (Otto and Simpson, 2006), after which the oxidation with CuO
285 preferentially yields mostly ether-bound monomers (Kaiser and Benner, 2012). A combination of the three approaches selectively broke down and extracted approximately 76% of the total biomass and 85% of the total carbon in roots (Fig. 2). The residue after the three-step sequential extraction contained mostly O-alkyl and di-O-alkyl carbon (Fig. 3), which was

widely attributed to the contribution of cellulose and hemicellulose (Foston, 2014). Our results suggest that the chemical depolymerization is a practical approach to obtaining carbon fractions from root biopolymers for further characterization.

290   Upon combining the GC-MS and FT-ICR MS, our results showed that the compositional carbon traits of fine roots after sequential chemical extraction were further supported by the ^{13}C-NMR data. For example, the results of ~~target~~targeted and non-~~target~~targeted approaches consistently indicated that the unsaturation degree and aromaticity of components increased from F_{DcMe} to F_{CuOox} (Fig. 4; Table ~~S4~~S5), which corresponded to a decrease in the alkyl carbon region from R1 to R2 and a further decrease in the carbonyl and carboxyl carbon, *O*-aromatic carbon, and aromatic carbon regions of residues from R2

295   to R4 (Fig. 3; Fig. S2). GC-MS results showed that based on the qualitative and quantitative detection of specific compounds in the extracted fractions, 78, 38, and 10 compounds were identified and quantified in F_{DcMe}, F_{KOHhy}, and F_{CuOox}, respectively (Fig. 4; Table ~~S1~~S2). As a complementary tool, ~~the~~FT-ICR MS is a non-targeted technique that has sufficient mass-resolving power to separate and accurately assign elemental compositions to individual molecules (Qi et al., 2022; He et al., 2022). FT-ICR MS spectra provided a total of 8631 assigned formulae in all samples (Fig. S3; Table ~~S3~~S4), which was

300   approximately 100 times more than the total number of components identified by GC-MS. In addition, a considerable number of nitrogen- and sulfur-containing compounds (CHON, CHOS, and CHONS) were also identified (Table ~~S4~~S5), which were not well captured by GC-MS. Therefore, concordant with our first hypothesis, the non-targeted and targeted analyses were consistent and complementary in showing analyte polarity and unsaturation degree after sequential chemical extraction. These two techniques combined with sequential chemical extraction significantly extended the analytical

305   windows of the compositional carbon traits of fine roots.

4.2 Different compositional carbon traits between SGR and WGR

Environmental stress elicits plant adaptive responses via the preferential biosynthesis and production of specific compounds from assimilated carbon, which provide efficient protection against specific stressors (Suseela and Tharayil, 2018). This study demonstrated that compared with SGR, WGR contained a high proportion of free compounds and free carbon (Fig. 2a,

310   b), specifically more free phenols, terpenoids, and steroids (Fig. ~~3a~~4a). It is consistent with a previous finding that plants exposed to environmental stress (including waterlogging) tended to produce more extractable labile compounds to counter the environmental imbalance than those growing in optimal conditions (Suseela and Tharayil, 2018). However, WGR contained less ash (Fig. ~~1c~~2c) and free organic acids than SGR (Fig. ~~2a~~4a). In general, one of the functions of endogenous organic acids in roots is to modulate the imbalance of cellular electroneutrality and osmotic pressure caused by a large

315   number of cations absorbed from the medium (Crawford and Tyler, 1969). The relatively lower concentrations of organic acids in WGR than in SGR tend to match the low solute concentration and low osmotic pressure in aquatic medium.

In addition, the whole plant structural matrix is notably altered under environmental stress (Le Gall et al., 2015), because many recalcitrant heteropolymers, including lignin and suberin phenolics, are biosynthesized via the phenylpropanoid pathway and can be directly regulated by environmental stressors (Dong and Lin, 2021)~~.~~, including flooding (Yamauchi et

320   al., 2019), drought and salt stresses (De Silva et al., 2021). Our results showed that compared with F_{KOHhy} of SGR, WGR's had higher average values of DBE, AI_{mod} and NOSC ($P < 0.05$; Table ~~S4~~S5) and more formulae (both specific and common formulae but had over 20% more relative intensity) with high O/C ratios and low H/C ratios (Fig. 5d-f), especially approximately twice more phenols ion F_{KOHhy} (Fig. ~~2b~~4b, Table ~~S1~~S2), indicating more biosynthesis and deposition of suberin phenolics (for example, ferulic acids) in WGR (Ranathunge et al., 2011). Although there were no significant

325   differences in the concentrations of eight lignin phenols in F_{CuOox} between two classes of roots (Fig. ~~4~~4c; Table ~~S2~~S3), F_{CuOox} of WGR had higher average values of DBE, AI_{mod} and NOSC ($P < 0.05$; Table ~~S4~~S5) and more formulae with high O/C ratios and low H/C ratios (Fig. 5g-i) than that of SGR. These were consisted with the previous study based on histochemistry and microscopy which suggested apoplastic barriers with suberin lamellae and secondary lignification in the cortex of fine roots could promote adaptation of *Metasequoia glyptostroboides* to aquatic environments (Yang et al., 2019). Moreover,

330   higher oxidation and carboxylation were observed in specific formulae of WGR (Fig. 6), suggesting increased oxidative stress and further regulation of the shikimate pathway under flooding conditions (Karlova et al., 2021; Dong and Lin, 2021).

Notably, the non-targeted analyses also showed that there were over two-thirds less quantity and abundance of sulfur-containing compounds (CHOS and CHONS) in WGR than in SGR ($P < 0.05$, Table ~~S4~~S5). It may be because the lower sulfur content in water than in soil resulted in reduced sulfur absorption and assimilation in plant roots (Hawkesford and De

335   Kok, 2006). Thus, it is necessary to monitor possible sulfur deficiencies in trees resulting from flooding-prone regions under future global environmental change.

In summary, our results partially supported the second hypothesis — waterlogging altered the distribution and accumulation of free and bound components. The waterlogging tends to increase free carbon fractions (especially free phenols, terpenoids, and steroids) and bound carbon fractions (e.g., bond phenols and V:$\Lambda 8$ ratio) but decrease the contents of free organic acids,

340   bond aliphatics, and the S:$\Lambda 8$ ratio in lignin-derived phenols, supporting that plants remarkably regulate biomass and carbon partitioning under changing environments (Karlova et al., 2021).

~~4.3 Ecological implications~~

4.3 Impact of molecular-level carbon traits of fine roots to decomposition

Plant organic matter is the most important source of soil organic carbon pool. The environmental condition was a key factor

345   affecting litter decomposition (Table ~~S5~~S7). In this study, fine roots had slower decomposition rates of carbon in anoxic conditions than in aerobic conditions (Fig. 7). Similar to our findings, many studies also observed a general negative effect of O_2 limitation on aerobic respiration (Larowe and Van Cappellen, 2011) and organic matter decomposition in soil (Kirschbaum et al., 2021; Sjogaard et al., 2017), wetlands (Lacroix et al., 2019), and marine sediment (Jessen et al., 2017). Moreover, environmental stressors can alter the structure and metabolic activity of the decomposer community (Chuckran et

350   al., 2020). For example, flooding of soils induced the function increase of CH_4 production, S cycle, and Fe cycle (e.g., *Bathyarchaeota*, *Bacteroidetes*, and *Geobacter*) and the function decrease of environmental remediation and biological

control (e.g., *Blastococcus* and *Roseiflexus*) (Luo et al., 2023), which consequently regulated organic carbon sequestration and biogeochemical cycling.

Our observation that decomposition was also strongly affected by root type (Table S5S7) supports the view that litter properties were one of the overriding factors in decomposition (Huys et al., 2022; Rummel et al., 2020). Contrary to hypothesis 3, our short-term root decomposition study showed that. Although conventional wisdom held that high specific root length and lower carbon nitrogen ratio commonly correlated with fast decomposition rates (Guo et al., 2021), our decomposition experiment exhibited the organic carbon decomposability was higher in WGR with lower specific root length and higher carbon nitrogen ratio than in SGR (Fig. 7, Table S6). Therefore, the commonly used parameters like morphological traits and stoichiometric indicators can not well predict the decomposition characteristics of fine roots under flooded conditions. In addition, contrary to hypothesis 3, WGR with more phenolics and higher unsaturation degree and aromaticity experienced nearly 15% more carbon loss than SGR after 180 days of incubation (Fig. 7). That is to say, the higher bound phenolics in WGR than in SGR could not explain the faster organic carbon decomposition in WGR than in SGR. Instead, the high carbon content in the free fraction in WGR than in SGR (F_{DcMe}, Fig. 2) was likely the major reason. It conformed to the previous conceptual model, which suggested that free organic carbon and non-structural compounds controlled the amount of litter-C lost in the early and middle decomposition phase (Soong et al., 2015; Shipley and Tardif, 2021). Moreover, WGR exhibited consistently higher decomposability of organic carbon than SGR in anoxic conditions, approaching the carbon decomposition potential of SGR in aerobic conditions (Fig. 7). The result suggested that although flooding provided an anoxic condition that slowed down root decomposition, the adaptive strategy of developing more non-structural labile tissue components in WGR to flooding would accelerate root decomposition to counteract the effect of anoxic condition.

5 Conclusions

This study developed and applied the complementary targeted and non-targeted analyses of sequentially extracted fractions of fine roots to determine the molecular-level fine-root carbon traits. The sequential chemical extraction allowed the analyses of both non-structural and structural (e.g., biopolymers) root carbon components, and the combination of GC MS and FT-ICR MS analyses successfully provided complementary quantitative and qualitative compositional information on organic compounds. This combined method was applied to further reveal the distinct differences in molecular-level carbon traits between SGR and WGR. The targeted and non-targeted analyses were sufficiently sensitive to show that WGR was enriched in more phenolics with a higher unsaturation degree and aromaticity and a more non-structural composition to help plants cope with flooding stress than SGR. Also, we highlight that although flooding provided an anoxic condition that slowed down root decomposition in the short-term, the adaptive strategy of developing more non-structural labile tissue components in WGR to flooding would accelerate short-term root decomposition to counteractcounteracting the effect of anoxic conditions. Nevertheless, the long-term effects of chemical adaptation under flooded environments on root degradation and

carbon biogeochemical processes still require further evaluation. Together, we ~~validated~~incorporated the ~~complementarity of~~ ~~GC MS and FT ICR MS in the analysis of~~ molecular-level carbon traits of fine roots into trait-based ecology, which could greatly expand the root trait pools and thereby improve our understanding of plant functioning and biogeochemical progress in response to global environmental change.

Data availability

The data that support the findings of this study are available from Figshare Repository https://figshare.com/s/36443d5092cd73087eb0~~https://figshare.com/s/395094a24e35301b7e0d~~. Correspondence and requests for materials should be addressed to Junjian Wang.

Author contributions

M.W., S.K. and J.W. designed the experiment and wrote the manuscript; M.W., P.Z., H.L., G.D. and D.K. conducted the fieldwork and laboratory work; M.W. and P.Z. took part in statistical analysis. All authors, especially D.K. and J.W. contributed to further revising of the manuscript.

Competing interests

The contact author has declared that none of the authors has any competing interests.

Acknowledgements

This work was financially supported by the National Natural Science Foundation of China (42122054 ~~and,~~ 42192513, and 42321004), Key Platform and Scientific Research Projects of Guangdong Provincial Education Department (2019KZDXM028 and 2020KCXTD006), Guangdong Basic and Applied Basic Research Foundation (2021B1515020082), Shenzhen Science & Technology Project (KCXFZ20201221173612033), and School level technical research project (SZIIT2022KJ081 and LHPY—2019017).

References

Agethen, S. and Knorr, K.-H.: Juncus effusus mono-stands in restored cutover peat bogs – Analysis of litter quality, controls of anaerobic decomposition, and the risk of secondary carbon loss, Soil Biol. Biochem., 117, 139-152, https://doi.org/10.1016/j.soilbio.2017.11.020, 2018.

Augusto, L. and Boca, A.: Tree functional traits, forest biomass, and tree species diversity interact with site properties to drive forest soil carbon, Nat. Commun., 13, 1097, https://doi.org/10.1038/s41467-022-28748-0, 2022.

410   Bharate, S. B., Kumar, V., Jain, S. K., Mintoo, M. J., Guru, S. K., Nuthakki, V. K., Sharma, M., Bharate, S. S., Gandhi, S. G., Mondhe, D. M., Bhushan, S., and Vishwakarma, R. A.: Discovery and Preclinical Development of IIIM-290, an Orally Active Potent Cyclin-Dependent Kinase Inhibitor, J. Med. Chem., 61, 1664-1687, https://doi.org/10.1021/acs.jmedchem.7b01765, 2018.

Chuckran, P. F., Reibold, R., Throop, H. L., and Reed, S. C.: Multiple mechanisms determine the effect of warming on plant litter decomposition in a dryland, Soil Biol. Biochem., 145, 107799, https://doi.org/10.1016/j.soilbio.2020.107799, 2020.

415   Coffin, A. and Ready, J. M.: Selective Synthesis of (+)-Dysoline, Org. Lett., 21, 648-651, https://doi.org/10.1021/acs.orglett.8b03777, 2019.

Colmer, T. D., Kotula, L., Malik, A. I., Takahashi, H., Konnerup, D., Nakazono, M., and Pedersen, O.: Rice acclimation to soil flooding: Low concentrations of organic acids can trigger a barrier to radial oxygen loss in roots, Plant, Cell Environ., 42, 2183-2197, https://doi.org/10.1111/pce.13562, 2019.

420   Cornelissen, J. H. C., Cornwell, W. K., Freschet, G. T., Weedon, J. T., Berg, M. P., and Zanne, A. E.: Coevolutionary legacies for plant decomposition, Trends Ecol. Evol., 38, 44-54, https://doi.org/10.1016/j.tree.2022.07.008, 2023.

Crawford, R. M. and Tyler, P. D.: Organic acid metabolism in relation to flooding tolerance in roots, J. Ecol., 57, 235-244, https://doi.org/10.2307/2258217, 1969.

de Silva, N. D. G., Murmu, J., Chabot, D., Hubbard, K., Ryser, P., Molina, I., and Rowland, O.: Root Suberin Plays Important Roles in Reducing Water Loss and Sodium Uptake in Arabidopsis thaliana, Metabolites, 11, 735, 2021.

425

Dijkstra, F. A., Zhu, B., and Cheng, W.: Root effects on soil organic carbon: a double-edged sword, New Phytol., 230, 60-65, https://doi.org/10.1111/nph.17082, 2021.

Dong, N. Q. and Lin, H. X.: Contribution of phenylpropanoid metabolism to plant development and plant-environment interactions, J. Integr. Plant Biol., 63, 180-209, https://doi.org/10.1111/jipb.13054, 2021.

430   Feng, X. J., Simpson, A. J., Wilson, K. P., Williams, D. D., and Simpson, M. J.: Increased cuticular carbon sequestration and lignin oxidation in response to soil warming, Nat. Geosci., 1, 836-839, https://doi.org/10.1038/ngeo361, 2008.

Foston, M.: Advances in solid-state NMR of cellulose, Curr. Opin. Biotechnol., 27, 176-184, https://doi.org/10.1016/j.copbio.2014.02.002, 2014.

Freschet, G. T., Roumet, C., Comas, L. H., Weemstra, M., Bengough, A. G., Rewald, B., Bardgett, R. D., De Deyn, G. B., Johnson, D.,
435   Klimesova, J., Lukac, M., McCormack, M. L., Meier, I. C., Pages, L., Poorter, H., Prieto, I., Wurzburger, N., Zadworny, M., Bagniewska-Zadworna, A., Blancaflor, E. B., Brunner, I., Gessler, A., Hobbie, S. E., Iversen, C. M., Mommer, L., Picon-Cochard, C., Postma, J. A., Rose, L., Ryser, P., Scherer-Lorenzen, M., Soudzilovskaia, N. A., Sun, T., Valverde-Barrantes, O. J., Weigelt, A., York, L. M., and Stokes, A.: Root traits as drivers of plant and ecosystem functioning: current understanding, pitfalls and future research needs, New Phytol., 232, 1123-1158, 10.1111/nph.17072, 2021a.

440   Freschet, G. T., Pages, L., Iversen, C. M., Comas, L. H., Rewald, B., Roumet, C., Klimesova, J., Zadworny, M., Poorter, H., Postma, J. A., Adams, T. S., Bagniewska-Zadworna, A., Bengough, A. G., Blancaflor, E. B., Brunner, I., Cornelissen, J. H. C., Garnier, E., Gessler, A., Hobbie, S. E., Meier, I. C., Mommer, L., Picon-Cochard, C., Rose, L., Ryser, P., Scherer-Lorenzen, M., Soudzilovskaia, N. A., Stokes, A., Sun, T., Valverde-Barrantes, O. J., Weemstra, M., Weigelt, A., Wurzburger, N., York, L. M., Batterman, S. A., Gomes de Moraes, M., Janecek, S., Lambers, H., Salmon, V., Tharayil, N., and McCormack, M. L.: A starting guide to root ecology: strengthening
445   ecological concepts and standardising root classification, sampling, processing and trait measurements, New Phytol., 232, 973-1122, 10.1111/nph.17572, 2021b.

Guo, L. L., Deng, M. F., Yang, S., Liu, W. X., Wang, X., Wang, J., and Liu, L. L.: The coordination between leaf and fine root litter decomposition and the difference in their controlling factors, Global Ecology and Biogeography, 30, 2286-2296, 10.1111/geb.13384, 2021.

450   Hawkesford, M. J. and De Kok, L. J.: Managing sulphur metabolism in plants, Plant, Cell Environ., 29, 382-395, https://doi.org/10.1111/j.1365-3040.2005.01470.x, 2006.

He, C., He, D., Chen, C. M., and Shi, Q.: Application of Fourier transform ion cyclotron resonance mass spectrometry in molecular characterization of dissolved organic matter, Science China-Earth Sciences, 65, https://doi.org/10.1007/s11430-021-9954-0, 2022.

Herzog, M., Striker, G. G., Colmer, T. D., and Pedersen, O.: Mechanisms of waterlogging tolerance in wheat--a review of root and shoot
455   physiology, Plant, Cell Environ., 39, 1068-1086, https://doi.org/10.1111/pce.12676, 2016.

Huys, R., Poirier, V., Bourget, M. Y., Roumet, C., Hattenschwiler, S., Fromin, N., Munson, A. D., and Freschet, G. T.: Plant litter chemistry controls coarse-textured soil carbon dynamics, J. Ecol., 110, 2911-2928, https://doi.org/10.1111/1365-2745.13997, 2022.

Iqbal, J., Hu, R., Lin, S., Ahamadou, B., and Feng, M.: Carbon dioxide emissions from Ultisol under different land uses in mid–subtropical China, Geoderma, 152, 63-73, https://doi.org/10.1016/j.geoderma.2009.05.011, 2009.

460   Jessen, G. L., Lichtschlag, A., Ramette, A., Pantoja, S., Rossel, P. E., Schubert, C. J., Struck, U., and Boetius, A.: Hypoxia causes preservation of labile organic matter and changes seafloor microbial community composition (Black Sea), Sci. Adv., 3, e1601897, https://doi.org/10.1126/sciadv.1601897, 2017.

Jing, H., Wang, H., Wang, G., Liu, G., and Cheng, Y.: Hierarchical traits of rhizosphere soil microbial community and carbon metabolites of different diameter roots of Pinus tabuliformis under nitrogen addition, Carbon Research, 2, 47, 10.1007/s44246-023-00081-1, 2023.

465 Kaiser, K. and Benner, R.: Characterization of lignin by gas chromatography and mass spectrometry using a simplified CuO oxidation method, Anal. Chem., 84, 459-464, https://doi.org/10.1021/ac202004r, 2012.

Karlova, R., Boer, D., Hayes, S., and Testerink, C.: Root plasticity under abiotic stress, Plant Physiol., 187, 1057-1070, https://doi.org/10.1093/plphys/kiab392, 2021.

Kellerman, A. M., Kothawala, D. N., Dittmar, T., and Tranvik, L. J.: Persistence of dissolved organic matter in lakes related to its
470 molecular characteristics, Nat. Geosci., 8, 454-457, https://doi.org/10.1038/ngeo2440, 2015.

Khatami, S., Deng, Y., Tien, M., and Hatcher, P. G.: Formation of water-soluble organic matter through fungal degradation of lignin, Org. Geochem., 135, 64-70, https://doi.org/10.1016/j.orggeochem.2019.06.004, 2019.

Kirschbaum, M. U. F., Don, A., Beare, M. H., Hedley, M. J., Pereira, R. C., Curtin, D., McNally, S. R., and Lawrence-Smith, E. J.: Sequestration of soil carbon by burying it deeper within the profile: A theoretical exploration of three possible mechanisms, Soil Biol.
475 Biochem., 163, 108432, https://doi.org/10.1016/j.soilbio.2021.108432, 2021.

Koch, B. P. and Dittmar, T.: From mass to structure: An aromaticity index for high-resolution mass data of natural organic matter, Rapid Commun. Mass Spectrom., 20, 926-932, https://doi.org/10.1002/rcm.2386, 2006.

Koch, B. P. and Dittmar, T.: From mass to structure: an aromaticity index for high-resolution mass data of natural organic matter, Rapid Commun. Mass Spectrom., 30, 250-250, https://doi.org/10.1002/rcm.7433, 2016.

480 Kotula, L., Ranathunge, K., Schreiber, L., and Steudle, E.: Functional and chemical comparison of apoplastic barriers to radial oxygen loss in roots of rice (*Oryza sativa* L.) grown in aerated or deoxygenated solution, J. Exp. Bot., 60, 2155-2167, https://doi.org/10.1093/jxb/erp089, 2009.

Kujawinski, E. B. and Behn, M. D.: Automated analysis of electrospray ionization fourier transform ion cyclotron resonance mass spectra of natural organic matter, Anal. Chem., 78, 4363-4373, https://doi.org/10.1021/ac0600306, 2006.

485 LaCroix, R. E., Tfaily, M. M., McCreight, M., Jones, M. E., Spokas, L., and Keiluweit, M.: Shifting mineral and redox controls on carbon cycling in seasonally flooded mineral soils, Biogeosciences, 16, 2573-2589, https://doi.org/10.5194/bg-16-2573-2019, 2019.

LaRowe, D. E. and Van Cappellen, P.: Degradation of natural organic matter: A thermodynamic analysis, Geochim. Cosmochim. Acta, 75, 2030-2042, https://doi.org/10.1016/j.gca.2011.01.020, 2011.

Le Gall, H., Philippe, F., Domon, J. M., Gillet, F., Pelloux, J., and Rayon, C.: Cell wall metabolism in response to abiotic stress, Plants
490 (Basel), 4, 112-166, https://doi.org/10.3390/plants4010112, 2015.

Luo, S., Jia, Z., Tian, L., Wang, S., Chang, C., Ji, L., Chang, J., Zhang, J., and Tian, C.: Potential functional differentiation from microbial perspective under dryland-paddy conversion in black soils, Agric. Ecosyst. Environ., 353, 10.1016/j.agee.2023.108562, 2023.

Macabuhay, A., Arsova, B., Walker, R., Johnson, A., Watt, M., and Roessner, U.: Modulators or facilitators? Roles of lipids in plant root-microbe interactions, Trends Plant Sci., 27, 180-190, https://doi.org/10.1016/j.tplants.2021.08.004, 2022.

495 Mann, M. E., Rahmstorf, S., Kornhuber, K., Steinman, B. A., Miller, S. K., Petri, S., and Coumou, D.: Projected changes in persistent extreme summer weather events: The role of quasi-resonant amplification, Sci. Adv., 4, eaat3272, https://doi.org/10.1126/sciadv.aat3272, 2018.

Martens, D. A.: Identification of phenolic acid composition of alkali-extracted plants and soils, Soil Sci. Soc. Am. J., 66, 1240-1248, https://doi.org/10.2136/sssaj2002.1240, 2002.

500 McCormack, M. L., Dickie, I. A., Eissenstat, D. M., Fahey, T. J., Fernandez, C. W., Guo, D., Helmisaari, H. S., Hobbie, E. A., Iversen, C. M., Jackson, R. B., Leppalammi-Kujansuu, J., Norby, R. J., Phillips, R. P., Pregitzer, K. S., Pritchard, S. G., Rewald, B., and Zadworny, M.: Redefining fine roots improves understanding of below-ground contributions to terrestrial biosphere processes, New Phytol., 207, 505-518, https://doi.org/10.1111/nph.13363, 2015.

Mueller, K. E., Polissar, P. J., Oleksyn, J., and Freeman, K. H.: Differentiating temperate tree species and their organs using lipid
505 biomarkers in leaves, roots and soil, Org. Geochem., 52, 130-141, https://doi.org/10.1016/j.orggeochem.2012.08.014, 2012.

Nelson, P. N. and Baldock, J. A.: Estimating the molecular composition of a diverse range of natural organic materials from solid-state ^{13}C NMR and elemental analyses, Biogeochemistry, 72, 1-34, https://doi.org/10.1007/s10533-004-0076-3, 2005.

Otto, A. and Simpson, M. J.: Sources and composition of hydrolysable aliphatic lipids and phenols in soils from western Canada, Org. Geochem., 37, 385-407, https://doi.org/10.1016/j.orggeochem.2005.12.011, 2006.

510 Otto, A. and Simpson, M. J.: Analysis of soil organic matter biomarkers by sequential chemical degradation and gas chromatography-mass spectrometry, J. Sep. Sci., 30, 272-282, https://doi.org/10.1002/jssc.200600243, 2007.

Pedersen, O., Sauter, M., Colmer, T. D., and Nakazono, M.: Regulation of root adaptive anatomical and morphological traits during low soil oxygen, New Phytol., 229, 42-49, https://doi.org/10.1111/nph.16375, 2021.

Qi, Y., Xie, Q., Wang, J.-J., He, D., Bao, H., Fu, Q.-L., Su, S., Sheng, M., Li, S.-L., Volmer, D. A., Wu, F., Jiang, G., Liu, C.-Q., and Fu,
515 P.: Deciphering dissolved organic matter by Fourier transform ion cyclotron resonance mass spectrometry (FT-ICR MS): from bulk to fractions and individuals, Carbon Research, 1, 3, https://doi.org/10.1007/s44246-022-00002-8, 2022.

Ranathunge, K., Schreiber, L., and Franke, R.: Suberin research in the genomics era-New interest for an old polymer, Plant Sci., 180, 399-413, https://doi.org/10.1016/j.plantsci.2010.11.003, 2011.

Rummel, P. S., Pfeiffer, B., Pausch, J., Well, R., Schneider, D., and Dittert, K.: Maize root and shoot litter quality controls short-term CO_2 and N_2O emissions and bacterial community structure of arable soil, Biogeosciences, 17, 1181-1198, https://doi.org/10.5194/bg-17-1181-2020, 2020.

Shipley, B. and Tardif, A.: Causal hypotheses accounting for correlations between decomposition rates of different mass fractions of leaf litter, Ecology, 102, https://doi.org/10.1002/ecy.3196, 2021.

Sjogaard, K. S., Treusch, A. H., and Valdemarsen, T. B.: Carbon degradation in agricultural soils flooded with seawater after managed coastal realignment, Biogeosciences, 14, 4375-4389, https://doi.org/10.5194/bg-14-4375-2017, 2017.

Soong, J. L., Parton, W. J., Calderon, F., Campbell, E. E., and Cotrufo, M. F.: A new conceptual model on the fate and controls of fresh and pyrolized plant litter decomposition, Biogeochemistry, 124, 27-44, https://doi.org/10.1007/s10533-015-0079-2, 2015.

Sun, T., Hobbie, S. E., Berg, B., Zhang, H., Wang, Q., Wang, Z., and Hattenschwiler, S.: Contrasting dynamics and trait controls in first-order root compared with leaf litter decomposition, Proc. Natl. Acad. Sci. U. S. A., 115, 10392-10397, https://doi.org/10.1073/pnas.1716595115, 2018.

Suseela, V. and Tharayil, N.: Decoupling the direct and indirect effects of climate on plant litter decomposition: Accounting for stress-induced modifications in plant chemistry, Glob. Chang. Biol., 24, 1428-1451, https://doi.org/10.1111/gcb.13923, 2018.

Tolić, N., Liu, Y., Liyu, A., Shen, Y., Tfaily, M. M., Kujawinski, E. B., Longnecker, K., Kuo, L.-J., Robinson, E. W., Paša-Tolić, L., and Hess, N. J.: Formularity: Software for automated formula assignment of natural and other organic matter from ultrahigh-resolution mass spectra, Anal. Chem., 89, 12659-12665, https://doi.org/10.1021/acs.analchem.7b03318, 2017.

Waggoner, D. C. and Hatcher, P. G.: Hydroxyl radical alteration of HPLC fractionated lignin: Formation of new compounds from terrestrial organic matter, Org. Geochem., 113, 315-325, https://doi.org/10.1016/j.orggeochem.2017.07.011, 2017.

Wang, M.K., Kong, D.L., Mo, X.H., Wang, Y.H., Yang, Q.P., Kardol, P., Valverde-Barrantes, O.J., Simpson, M.J., Zeng, H., Reich, P.B., Bergmann, J., Tharayil, N., Wang, J.J.: Molecular-level carbon traits underlie multi-dimensional fine root economics space, Nat. Plants, Accepted, 2024.

Wang, J. J., Tharayil, N., Chow, A. T., Suseela, V., and Zeng, H.: Phenolic profile within the fine-root branching orders of an evergreen species highlights a disconnect in root tissue quality predicted by elemental- and molecular-level carbon composition, New Phytol., 206, 1261-1273, https://doi.org/10.1111/nph.13385, 2015.

Wang, Y. H., Liu, Y. A., Chu, R. K., Bowden, R. D., Lajtha, K., Simpson, M. J., and Wang, J. J.: Characterization of sequentially extracted soil organic matter by electrospray ionization and atmospheric pressure photoionization Fourier transform ion cyclotron resonance mass spectrometry, ACS Earth Space Chem., 6, 2142-2148, https://doi.org/10.1021/acsearthspacechem.2c00180, 2022.

Wen, X.-F., Yu, G.-R., Sun, X.-M., Li, Q.-K., Liu, Y.-F., Zhang, L.-M., Ren, C.-Y., Fu, Y.-L., and Li, Z.-Q.: Soil moisture effect on the temperature dependence of ecosystem respiration in a subtropical Pinus plantation of southeastern China, Agric. For. Meteorol., 137, 166-175, https://doi.org/10.1016/j.agrformet.2006.02.005, 2006.

Wild, B., Shakhova, N., Dudarev, O., Ruban, A., Kosmach, D., Tumskoy, V., Tesi, T., Grimm, H., Nybom, I., Matsubara, F., Alexanderson, H., Jakobsson, M., Mazurov, A., Semiletov, I., and Gustafsson, O.: Organic matter composition and greenhouse gas production of thawing subsea permafrost in the Laptev Sea, Nat. Commun., 13, 5057, https://doi.org/10.1038/s41467-022-32696-0, 2022.

Yamauchi, T., Abe, F., Tsutsumi, N., and Nakazono, M.: Root cortex provides a venue for gas-space formation and is essential for plant adaptation to waterlogging, Front. Plant Sci., 10, 259, https://doi.org/10.3389/fpls.2019.00259, 2019.

Yamauchi, T., Pedersen, O., Nakazono, M., and Tsutsumi, N.: Key root traits of Poaceae for adaptation to soil water gradients, New Phytol., 229, 3133-3140, https://doi.org/10.1111/nph.17093, 2021.

Yang, C., Zhang, X., Wang, T., Hu, S., Zhou, C., Zhang, J., and Wang, Q.: Phenotypic plasticity in the structure of fine adventitious metasequoia glyptostroboides roots allows adaptation to aquatic and terrestrial environments, Plants (Basel), 8, 501, https://doi.org/10.3390/plants8110501, 2019.